

1 **Title: The hypomethylation of imprinted genes in IVF/ICSI placenta samples is**
2 **associated with concomitant changes in histone modifications**

3

4 **Running title:** Methylation changes are associated with histone modifications in IVF-
5 placentas

6

7 Cécile Choux^{1,2,*} (MD-PhD), Paolo Petazzi³ (PhD), Marta Sanchez-Delgado³ (PhD), José R.
8 Hernandez Mora³ (PhD), Ana Monteagudo³ (PhD), Paul Sagot² (MD), David Monk^{3,4} (PhD),
9 Patricia Fauque^{1,5} (MD, PhD)

10

11 ¹ Université Bourgogne Franche-Comté - INSERM UMR1231, F-21000 Dijon, France

12 ² CHU Dijon Bourgogne, Service de Gynécologie-Obstétrique, F-21000 Dijon, France

13 ³ Imprinting and Cancer group, Cancer Epigenetic and Biology Program, Bellvitge Biomedical
14 Research Institute, 08908 L'Hospitalet de Llobregat, Barcelona, Spain

15 ⁴ Biomedical Research Centre, University of East Anglia, Norwich Research Park, Norwich
16 Norfolk, NR4 7TJ, UK

17 ⁵ CHU Dijon Bourgogne, Laboratoire de Biologie de la Reproduction, F-21000 Dijon, France

18

19

20

21

22 ***ADDRESS CORRESPONDENCE TO:**

23 Dr Cécile Choux, MD-PhD

24 Service de Gynécologie et Biologie de la Reproduction

25 CHU Dijon - BP 77908

26 14, rue Gaffarel

27 21079 DIJON CEDEX

28 Tel (Office): +333-80-29-36-14

29 Tel (Lab): +333-80-29-51-01

30 Fax: +333-80-29-51-16

31 cecile.choux@chu-dijon.fr

32 **Abstract**

33 Although more and more children are born by Assisted Reproductive Technologies (ART),
34 ART safety has not fully been demonstrated. Notably, ART could disturb the delicate step of
35 implantation, and trigger placenta-related adverse outcomes with potential long-term effects,
36 through disrupted epigenetic regulation. We have previously demonstrated that placental
37 DNA methylation was significantly lower after IVF/ICSI than following natural conception at
38 two differentially methylated regions (DMRs) associated with imprinted genes (IGs):
39 *H19/IGF2* and *KCNQ1OT1*. As histone modifications are critical for placental physiology, the
40 aim of this study was to profile permissive and repressive histone marks in placenta biopsies
41 to reveal a better understanding of the epigenetic changes in the context of ART. Utilizing
42 chromatin immunoprecipitation (ChIP) coupled with quantitative PCR, permissive (H3K4me3,
43 H3K4me2 and H3K9ac) and repressive (H3K9me3 and H3K9me2) post-translational histone
44 modifications were quantified. The analyses revealed significantly higher quantity of
45 H3K4me2 precipitation in the IVF/ICSI group than in the natural conception group for
46 *H19/IGF2* and *KCNQ1OT1* DMRs (P = 0.016 and 0.003, respectively). Conversely, the
47 quantity of both repressive marks at *H19/IGF2* and *SNURF* DMRs was significantly lower in
48 the IVF/ICSI group than in the natural conception group (P = 0.011 and 0.027 for *H19/IGF2*;
49 and P = 0.010 and 0.035 for *SNURF*). These novel findings highlight that DNA
50 hypomethylation at imprinted DMRs following ART is linked with increased
51 permissive/decreased repressive histones marks, altogether promoting a more permissive
52 chromatin conformation. This concomitant change in epigenetic state at IGs at birth might be
53 an important developmental event because of ART manipulations.

54

55 **Keywords:** Assisted reproductive technologies, epigenetics, histone modifications, *in vitro*
56 fertilization, DNA methylation, placenta

57 **Introduction**

58

59 It is estimated that more than six million children have been born by Assisted Reproductive
60 Technologies (ART) worldwide, representing ~4% of all births [1,2]. However, the safety of
61 these techniques has not fully been demonstrated. ART has been associated with an
62 increased risk of placenta-related adverse pregnancy, perinatal outcomes and imprinting
63 disorders [3-6]. As ART take place during the epigenetic-sensitive period of preimplantation
64 when genome-wide erasure and selective reprogramming occur, these techniques could
65 affect the implantation step, when the dialogue between endometrium and embryo
66 establishes the placental invasion into the uterine wall [7]. Together, these data raise the
67 concern of the potential epigenetic vulnerability associated with ART.

68 Epigenetic mechanisms have been demonstrated to have a fundamental role in regulating
69 placental function [7]. Notably, imprinted genes (IGs) are known to modulate foetal and
70 placental growth, for example by regulating nutrients transfer, cell cycle and insulin
71 metabolism [8-10]. Among imprinting mechanisms, DNA methylation in human placenta has
72 been extensively studied, but literature about histone modifications after ART is relatively
73 scarce. Modifications of basic histone amino (N)-terminal tail lead to changes in the overall
74 chromatin structure and in the binding of effector molecules [11] and thus changes regulation
75 of DNA transcription, replication, recombination and repair. For example, acetylation of the
76 lysine 9 of histone H3 (H3K9ac) neutralizes the positive charge of histone H3, decreasing the
77 histone's affinity to bind DNA, resulting in a more "relaxed" chromatin state which is
78 permissive to gene expression. More complex than acetylation, histone methylation can be
79 either a permissive or a repressive mark, according to its location on the histone tail. Though
80 tri-methylation of lysine 4 on histone H3 (H3K4me3) is permissive, tri-methylation of lysine 9
81 on histone H3 is repressive when located in the promoters regions [12]. A wealth of data
82 have underlined that histone modifications are critical for trophoblast establishment [13] and
83 placental physiology [14]. Notably, chronic ischemia in the rodent placenta was linked to

84 decreased histone H3 acetylation levels [15]. In human, abnormal histone methylation at
85 some imprinted DMRs was linked with the development of placental disorders such as
86 preeclampsia and molar pregnancy [16]. Moreover, the interest of studying histone
87 modifications in the context of ART is reinforced by the fact that histone marks could be
88 disturbed by environmental stressors [17] and thus could mediate long-term health effects of
89 ART.

90 We previously demonstrated that DNA methylation in the placenta was significantly lower
91 after IVF/ICSI than following natural conception at two imprinted DMRs: *H19/IGF2* and
92 *KCNQ1OT1* [18]. The aim of this study was to determine whether DNA hypomethylation
93 could be associated with specific histones profiles, to reveal a better understanding of the
94 epigenetic modifications in the context of ART.

95

96

97 **Materials and methods**

98

99 **Study population**

100 Patients were prospectively included from January 1st, 2013 to April 30th, 2015 in the
101 Department of Obstetrics, Gynaecology and Reproductive Biology at Dijon University
102 Hospital, France. “Natural conception” group included singleton pregnancies of women that
103 had conceived spontaneously within 1 year after stopping contraception. “IVF/ICSI” group
104 included singleton pregnancies achieved following fresh embryo transfer after two days of *in*
105 *vitro* culture. This cohort has previously been described [18] and used to compare the DNA
106 methylation, by pyrosequencing, of 51 IVF/ICSI vs. 48 placentas from natural conception for
107 three imprinted DMRs associated with the *H19/IGF2*:IG-DMR, *KCNQ1OT1*:TSS-DMR, and
108 *SNURF*:TSS-DMR, named according to the recommendations for nomenclature [19]. For the
109 present study, to determine whether DNA hypomethylation could be associated with specific

110 histones profiles, 16 placentas from the IVF/ICSI group who presented with below 5th
111 percentile for methylation for at least one of these DMRs were selected (Figure 1). They
112 were compared with 16 controls matched for parity, new-born's sex, and gestational age at
113 delivery. The controls were selected among the 48 women with natural pregnancy from the
114 previous study.

115

116 **Sample preparation**

117 Placenta samples (1 cm³) were extracted from the foetal side within 15 min after delivery,
118 washed twice in 0.9% NaCl before being snap frozen in liquid nitrogen and conserved at -
119 80°C.

120

121 **DNA methylation and expression**

122 Data for expression and DNA methylation experiments were obtained from our previous
123 publication using real-time PCR and pyrosequencing, respectively [18], and analysed on this
124 new cohort of 32 samples.

125

126 ***Histone modifications analyses by Chromatin ImmunoPrecipitation (ChIP)***

127 For the three imprinted DMRs previously analysed three permissive histone marks
128 (di/trimethylation of lysine 4 of histone H3, H3K4me2/3; acetylation of lysine 9 of histone H3,
129 H3K9ac) [20] and two repressive histone marks associated with heterochromatic states
130 (di/trimethylation of lysine 9 of histone H3, H3K9me2/3) [21,22] were studied.

131

132 ***Preparation of chromatin from placenta samples***

133 Approximately 2 grams of frozen placenta was rinsed two times in cold PBS and placed in
134 lysis tubes (Zymo Research BashingBeads Lysis Tubes - 0.5 mm) containing 1 mL buffer I
135 (0.5 M Tris-HCl pH 7.5, 0.5 M KCl, 2.5 M NaCl, 0.5 M MgCl₂, 25 mM EGTA, 0.3 M sucrose,
136 0.5 mM DTT, 0.1 mM PMSF, 3.6 ng/mL aprotinin, 5 mM sodium butyrate) and subject to
137 three intervals of agitation (90 sec, 5000 rpm) using a Precellys24 homogenizer (Bertin

138 technologies) with 5 minutes on ice between each agitation cycle. The cell suspension was
139 then placed in 7 mL of buffer II (buffer I with NP40 at a final concentration of 0.2%) to purify
140 nuclei by centrifugation at 8500 rpm/12720g for 20 minutes with low acceleration and low
141 deceleration on a sucrose gradient (8 mL from the previous step carefully placed on 25 mL of
142 buffer III (0.5 M Tris-HCl pH 7.5, 0.5 M KCl, 2.5 M NaCl, 0.5 M MgCl₂, 25 mM EGTA, 1.2 M
143 sucrose, 0.5 mM DTT, 0.1 mM PMSF, 3.6 ng/mL aprotinin, 5 mM sodium butyrate) in
144 Sorvall™ RC 6 Plus Centrifuge (ThermoScientific™). The nuclear pellet was resuspended in
145 digestion buffer (0.32 M sucrose, 50 mM Tris-HCl pH 7.5, 4 mM MgCl₂, 1mM CaCl₂, 0.1 mM
146 PMSF, 5mM sodium butyrate) to 0.4 mg DNA/mL (Quantification by absorbance). Aliquots of
147 500 µL were distributed in 1.5 mL tubes. Micrococcal nuclease (Nuclease S7 15 IU/µL,
148 Roche; final concentration 30 mIU/µL) was used to digest the chromatin to yield fragments
149 one to five nucleosomes in length, which typically presented an incubation time of 3 minutes
150 at 37°C. Digestion was stopped by adding 0.5 M EDTA at a final concentration of 20 mM and
151 cooling on ice. After centrifugation (10 min, 15800g, 4°C), the supernatant was designated
152 fraction S1. The pellet was resuspended in 500 µL lysis buffer (1 mM Tris-HCl pH 7.5, 0.2
153 mM EDTA, 0.2 mM PMSF, 5 mM sodium butyrate) and left 20-30 minutes on ice and subject
154 to a second centrifugation step (10 min, 15800g, 4°C), the supernatant of which was
155 designated fraction S2. The size of the nucleosomes was determined following Nucleospin
156 gel and PCR clean-up (Macherey-Nagel) of ~100 µL of each fraction, to ensure the S1
157 chromatin fraction mainly comprised of mono and dinucleosomes and the S2 poly-
158 nucleosomes of 2 to 5 nucleosomes (Supplemental Figure 1).

159

160 *Immunoprecipitation of fresh chromatin*

161 For ChIP, we used antibodies directed against H3K4me₃ (Diagenode C15410003-50),
162 H3K4me₂ (Millipore 07-030), H3K9ac (Cell Signaling 9649S), H3K9me₃ (Abcam AB8898),
163 H3K9me₂ (Diagenode C15410060) and a negative control (mock precipitation with mouse
164 IgG Millipore 12-371).

165 Chromatin was quantified by absorbance. For each condition, 4 µg of chromatin was used
166 (constituted of 75% S1 and 25% S2) and suspended in incubation buffer (20 mM Tris-HCl pH
167 7.5, 50 mM NaCl, 20 mM sodium butyrate, 5 mM EDTA, 0.1 mM PMSF) in a total volume of
168 500 µL for each condition. We precleared chromatin by agitating overnight at 4°C with 4%
169 Dynabeads® Protein G for immunoprecipitation (Invitrogen) washed three times in PBS-BSA
170 5%. In parallel, antibodies were combined to Dynabeads® Protein G for immunoprecipitation
171 (Invitrogen), each antibody being agitated overnight in 250 µL of PBS-BSA 5% containing
172 16% of beads previously washed three times in PBS-BSA 5%.

173 The following day, beads were removed from precleared chromatin and antibodies-beads
174 complexes were washed two times in PBS-BSA 5%. ChIP was then carried out for 4h at 4°C
175 The antibody-chromatin complexes were subsequently washed three times with each buffer
176 A (50 mM Tris-HCl, pH 7.5, 10 mM EDTA, 5 mM sodium butyrate, 75 mM NaCl), B (50 mM
177 Tris-HCl, pH 7.5, 10 mM EDTA, 5 mM sodium butyrate, 125 mM NaCl) and C (50 mM Tris-
178 HCl, pH 7.5, 10 mM EDTA, 5 mM sodium butyrate, 175 mM NaCl) to ensure only the fraction
179 of chromatin linked to the antibodies was retained. Elution was performed in 400 µL of elution
180 buffer (20 mM Tris-HCl pH 7.5, 50 mM NaCl, 5 mM EDTA, 1% SDS). After a digestion with
181 proteinase K (100 µg/mL) for 1 hour at 65°C, DNA was obtained from the input and bound
182 fractions with Nucleospin gel and PCR clean-up (Macherey-Nagel), according to the
183 manufacturer's protocol (protocol for samples SDS rich for bound fractions) with a final
184 elution with 40 µL of water.

185

186 *Quantification of immunoprecipitated chromatin*

187 For an initial check of precipitated DNA quality, allelic specificity PCR assays were performed
188 on all heterozygous samples. The PCR regions incorporated a Single Nucleotide
189 Polymorphisms (SNPs) to allow both alleles to be discriminated. PCR and direct sequencing
190 as used interrogate sequence traces, using Sequencher v4.6 (Gene Codes Corporation, MI).
191 Primers, PCR mix and conditions are available in Supplemental Table S1.

192

193 Levels of immunoprecipitated chromatin at each region of interest were determined by
194 quantitative real-time PCR amplification with the QuantStudio™ 5 Real-Time PCR system
195 (Applied Biosystems™), using the SYBR™ Green PCR Master Mix (Applied) (see
196 supplemental Table S2). Data were analysed with QuantStudio™ Design & Analysis
197 Software (v1.3.1). Each PCR was run in triplicate and level of immunoprecipitation was
198 quantified as a percentage of total input material as follows: % of input = $2^{(-\Delta Ct)}$ where ΔCt is
199 the difference in mean Ct triplicate between the DNA of interest and the DNA of the input.
200 To overcome the inherent variability of different immunoprecipitations, precipitation levels
201 obtained at the region of interest were normalized to the level obtained for positive control
202 intervals. Interrogation of placenta ChIP-seq datasets in the Genome Data viewer function in
203 the GEO data repository revealed that the promoter of *KLF10* was enriched for the
204 permissive histone marks H3K4me3, H3K4me2 and H3K9ac and was selected as a control
205 region. For a control of repressed chromatin, we selected a heterochromatic satellite region
206 on chromosome 4, which is ubiquitously associated with both H3K9me3 and H3K9me2.

207

208 ***Methylation-sensitive genotyping***

209 Approximately 500 ng of heterozygous placenta DNA was digested with 10 units of *HpaII* and
210 BstU1 restriction endonuclease for 6 hours at 37°C. The digested DNA was subject to
211 ethanol precipitation and resuspended in a final volume of 20 μ l TE. Approximately 50 ng of
212 digested DNA was used in each amplification reaction. The resulting amplicons were
213 sequenced, and the sequences traces were compared to those obtained for the
214 corresponding undigested DNA template.

215

216 **Statistical analyses**

217 Categorical variables were expressed as numbers (percentages) and compared using the
218 Chi-2 test or Fisher exact test when appropriate. Continuous variables were expressed as
219 means \pm standard deviations (SD) or medians and interquartile ranges [IQR] and compared
220 using the Student or Mann-Whitney test, as appropriate. Birth weights were normalized by

221 conversion to z-scores calculated using normal birthweight curves of our population
222 accounting for gestational age and new-born's sex [23]. Placental weights were also
223 converted into z-scores according to gestational age and new-born's sex [24]. All statistical
224 analyses were performed with SAS software, version 9.4 (SAS Institute Inc, USA). A two-
225 tailed $P < 0.05$ was considered significant.

226

227

228 **Results**

229 **Confirmation of *in-silico* histone modifications profiles in term placentas**

230 To ensure the PCR amplified intervals mapping to the imprinted DMRs were enriched for the
231 histone modification of interest, we performed an *in-silico* analysis to ensure primer design
232 coincided with the largest peaks in placenta-derived ChIP-seq datasets (GEO accession
233 numbers GSM1160199 for H3K4me3; GSM753439 for H3K4me2, GSM818049 for H3K9ac
234 and GSM1160204 for H3K9me3). Following primer optimization, amplicons of ~120-200bp,
235 which would allow for amplification of dinucleosome fragments and larger, were used to
236 quantify the precipitation levels for the three imprinted loci of interest: *H19/IGF2* (Figure 2A),
237 *KCNQ1OT1* (Figure 2B) and *SNURF* (Figure 2C) DMRs.

238 Subsequently we analysed the allelic precipitation of the ChIP material in the 16 naturally
239 conceived control samples, since we anticipated that permissive and repressive histone
240 marks should be on opposite parental alleles at these imprinted DMRs. PCR were performed
241 using primers that flanked highly informative SNPs and the resulting amplicons sequenced.
242 In total 9 samples were heterozygous for *H19/IGF2* (*rs2107425*), 9 for *KCNQ1OT1*
243 (*rs11023840*) and 9 for *rs4906939* within the *SNURF* DMR. The allelic precipitation levels
244 were compared to methylation-sensitive genotyping, which revealed that the permissive
245 marks were solely on the unmethylated allele and the repressive marks preferentially on the
246 opposite allele (Figure 3).

247

248 **Comparison between IVF/ICSI and natural conception groups**

249 The two groups were comparable in terms of parental and new-born characteristics (Table
250 1). As expected, the mean group DNA methylation of *H19/IGF2*, *KCNQ1OT1* and *SNURF*
251 DMRs was significantly lower in the IVF/ICSI group (45.1% [43.2-48.9]; 32.8% [31.7-35.7]
252 and 38.3% [35.5-40.5], respectively) compared to those conceived naturally (53.5% [49.6-
253 59.3], $P = 0.004$; 39.4% [34.8-41.9], $P = 0.001$ and 41.2% [38.4-42.1], $P = 0.036$,
254 respectively; Table 2, Figure 4A). Relative expression was not different between groups
255 (Table 2).

256 Quantitative PCR targeting *H19/IGF2* and *SNURF* DMRs in the H3K9me3 and H3K9me2
257 precipitated material revealed significantly lower quantities of H3K9me3 and H3K9me2 in the
258 IVF/ICSI group than in the natural conception group ($P = 0.011$ and 0.027 for *H19/IGF2*,
259 respectively; and $P = 0.010$ and 0.035 for *SNURF*, respectively; Figure 4B). There was no
260 significant difference for either repressive mark at *KCNQ1OT1* DMR (Figure 4B).

261 The quantity of H3K4me2 at *H19/IGF2* and *KCNQ1OT1* DMRs was significantly higher in the
262 IVF/ICSI group than in the natural conception group ($P = 0.016$ and 0.003 , respectively;
263 Figure 4C). There was no significant difference for H3K4me2 for *SNURF*, or for the other two
264 permissive marks (H3K4me3, H3K9ac; Figure 4C).

265 When the 8 conventional IVF cases were compared with the 8 IVF with ICSI, it showed that
266 there was no methylation difference between both groups (Supplemental Figure 2A).

267 However, the quantity of H3K9me3 at *KCNQ1OT1* DMR was significantly lower in the ICSI
268 than in the IVF group ($P = 0.032$; Supplemental Figure 2B), while the quantity of H3K4me2 in
269 the same interval was significantly higher in the ICSI than in the IVF group ($P = 0.003$;
270 Supplemental Figure 2C). There was no significant difference for the other permissive marks
271 H3K4me3 and H3K9ac, repressive mark H3K9me2, nor for the *SNRPN* and *H19/IGF2* DMRs
272 (Supplemental Figure 2).

273 One hypothesis that could explain the increased of permissive histone modifications in some
274 samples was the presence of these marks on the normally repressed allele. To address this,
275 we focused on the allelic precipitation profiles in IVF/ICSI samples with highest precipitation
276 levels (>75th percentile) of permissive marks at the *H19/IGF2* DMR. Sequencing of samples
277 heterozygous for SNPs revealed that the normally methylated allele was decorated with
278 H3K4me2 and H3K9ac (Supplemental Figure 3). However similar experiments targeting the
279 *KCNQ1OT1* and *SNURF* regions revealed maintained monoallelic precipitation patterns,
280 comparable to spontaneously conceived controls (Supplemental Figures 4 and 5,
281 respectively).

282

283

284 **Discussion**

285 These data demonstrate that DNA hypomethylation at imprinted DMRs could be associated
286 with an increase in permissive histone marks and/or with a decrease in repressive histone
287 modifications. This is consistent with a more “permissive” chromatin conformation on the
288 normally repressed allele. However, by focusing on outlier samples with highest precipitation
289 levels of permissive marks and heterozygous for SNPs, we observed the enrichment of
290 H3K4 methylation and H3K9 acetylation on the normally repressed and DNA methylated
291 allele at the *H19/IGF2* region. This suggests that some cells within the samples could lose
292 their allelic methylation and subsequently gained the permissive histone modifications. Single
293 cell studies, possibly incorporating Assay for Transposase-Accessible Chromatin using
294 sequencing (ATAC-seq) would be required to clarify this observation. In the *KCNQ1OT1* and
295 *SNURF* regions, *i.e.* maternally imprinted genes, the monoallelic imprint seemed to be
296 preserved.

297 Several studies have addressed the stability of DNA methylation in placenta after IVF. The
298 first reported lower DNA methylation levels in placentas after IVF than after natural

299 pregnancy [25], whilst other observed hypomethylation at the *MEST* and *H19* loci [25-27].
300 Our previous work evidenced lower DNA methylation levels of two imprinted loci (*H19/IGF2*
301 and *KCNQ1OT1*) and two transposable elements (LINE-1 and ERVFRD-1) in IVF placentas
302 while there was not any statistical difference between IVF and controls for *SNURF* DNA
303 methylation [18]. However not all studies have shown such clear-cut differences [28].
304 Concerning gene expression, higher levels of expression of some IGs such as *MEST* and
305 *H19* have been demonstrated after IVF [25,26], but other studies found lower expression
306 levels for *IGF2* and *H19* [29].
307 To our knowledge, this study is the first reporting altered post-translational histone
308 modification abundance in the human placenta after ART. Indeed, most studies focusing on
309 histone regulation have been conducted in mouse models and mainly in pre-implantation
310 embryos. For example, a study profiling epigenetic modifications at the *Mest* and *H19* loci in
311 mouse blastocysts cultured *in vitro* found an increased abundance of permissive histone
312 marks and a decrease in repressive histone modifications [21]. The same team confirmed
313 these trends at the *H19/Igf2* region on two cohorts of 2-cells embryos cultured *in vitro* until
314 the blastocyst stage or vitrified/thawed and then cultured *in vitro* until the blastocyst stage
315 [30]. Similarly, altered methylation of histones and DNA at the *H19/Igf2* region has also been
316 shown in embryonic stem cells derived from mice pre-implantation embryos [31].
317 Interestingly, in an IVF cattle model, a higher expression of the imprinted gene *PHLDA2* was
318 associated with an increase in the permissive mark H3K4me2 in its promoter [32]. Overall,
319 our results are consistent with those reported in these models.
320 The increased in permissive and decrease of repressive histones marks observed in our
321 study in hypomethylated samples following ART support the hypothesis that chromatin could
322 be more permissive to transcription. However, increased expression was evidenced neither
323 in this study nor in our previous one [18]. Nevertheless, as we worked on term placentas,
324 plasticity and adaptability of placenta to environment [7] suggest that the altered expression
325 could occur throughout pregnancy and no longer be visible at birth. This is well demonstrated
326 by increased *Igf2* expression after ART in superovulated mice placenta during gestation but

327 no longer visible at birth [33,34] and by the observation that a positive correlation between
328 placental *IGF2* expression and birth weight is only present during the first trimester and not at
329 term [35]. Indeed, as the placenta undergoes rapid epigenomic changes during gestation, a
330 placenta collected at birth may not reflect the changes occurring throughout pregnancy [17].
331 However, these epigenetic changes occurring during prenatal period, probably participating
332 in compensation mechanisms [7,18], raise questions about the potential long-term effects of
333 such modifications on children conceived by ART. As for the origin of these modifications,
334 recent studies showed that levels of histones mRNA could be different in infertile patients'
335 sperm compared to controls [36], and that H3K4me2 could be a molecular marker of sperm
336 quality [37], which raises questions about potential modifications in histones physiology
337 related to infertility. Moreover, increase in permissive and decrease in repressive histone
338 marks at *KCNQ1OT1* DMR in ICSI group compared to IVF group suggest that specific ICSI
339 protocols might influence histone regulation.

340 A limitation of this study could be the restricted number of IGs and histone marks studied. It
341 would be interesting to extend analyses to other imprinted DMRs as well as imprinted genes
342 with unmethylated promoters, regulated by neighbouring DMRs *in cis*, such as *CDKN1C* and
343 *PHLDA2* [22]. Furthermore, studying non-imprinted loci associated with early and late
344 placental development could be revealing. It would also be interesting to decipher the proper
345 roles of each placental cell type, although it would be technically difficult.

346

347

348 **Conclusion**

349 These novel findings highlight that DNA hypomethylation at imprinted DMRs after ART is
350 linked with increased permissive/decreased repressive histones marks, altogether promoting
351 an “permissive” conformation of the chromatin. This concomitant change in epigenetic state
352 at IGs at birth might be an important developmental event as a consequence of ART. To
353 date, exact causes and consequences of these changes are not known. Better knowledge of

354 the mechanisms at stake could enable to adapt our daily practice in order to reduce the
355 impact of these changes.

356

357 **Declarations**

358 **Ethics approval and consent to participate**

359 All women had given written informed consent in accordance with the Declaration of Helsinki.

360 The study was approved by the Institutional Review Board and the Ethics Committee of Dijon

361 University Hospital (*Comité de Protection des Personnes [CPP] Est I, n°2012-A01010-43*).

362

363 **Consent for publication**

364 Not applicable

365

366 **Availability of data and materials**

367 The datasets used and/or analysed during the current study are available from the

368 corresponding author on reasonable request

369

370 **Competing interests**

371 The authors declare that they have no competing interests.

372

373 **Funding**

374 This work was supported by Besançon and Dijon University Hospitals under grant “appel à

375 projet Dijon-Besançon 2013”, by the Agence Nationale pour la Recherche under grant “ANR-

376 17-CE12-0014” and by the Fonds pour la santé des femmes. The Monk laboratory was

377 supported by the Spanish Ministry of Economy and Competitiveness under grant “MINECO;

378 BFU2014-53093-R” and “BFU2017-85571-R” and by the European Union Regional

379 Development Fund (FEDER). A.M.S is a recipient of a FPI PhD studentship from MINECO.

380

381 **Authors' contributions**

382 PF, DM and CC were the principal investigators and take primary responsibility for the paper.
383 PF, DM, PP and CC were responsible for the study design. CC and PF recruited the patients.
384 CC, DM, PP, MS, JH and AM were involved in experiments. PF, DM and CC coordinated the
385 research. CC performed the statistical analyses. DM, PF and CC drafted the manuscript. All
386 authors read and approved the final manuscript.

387

388 **Acknowledgements**

389 We thank the midwives and nurses of Dijon University Hospital for their help in collecting
390 samples. We thank Benjamin Tournier and Laurence Jego for their help in optimizing
391 protocols. We thank Imprinting and Cancer group, Cancer Epigenetic and Biology Program,
392 Bellvitge Biomedical Research Institute for their help in realizing experiments. We thank
393 Sandrine Daniel, Marie-Laure Humbert-Asensio and Lydie Rossye (member of the "Centre
394 d'Investigation Clinique-Epidémiologie Clinique/essais cliniques" of Dijon) for their precious
395 help in monitoring and analysing the data. We thank Maud Carpentier of the "Direction de la
396 Recherche Clinique et de l'Innovation" (DRCI) of Dijon University Hospital for the promotion
397 and the management of the study. We thank Philip Bastable for his help in writing the
398 manuscript.

399

400

401

402

References

1. Messerlian C and Gaskins AJ. Epidemiologic Approaches for Studying Assisted Reproductive Technologies: Design, Methods, Analysis and Interpretation. *Curr Epidemiol Rep* 2017;(4):124-132.
2. Spaan M, van den Belt-Dusebout AW, van den Heuvel-Eibrink MM, Hauptmann M, Lambalk CB, Burger CW, et al. Risk of cancer in children and young adults conceived by assisted reproductive technology. *Hum Reprod* 2019;(34):740-750.
3. Lazaraviciute G, Kauser M, Bhattacharya S, and Haggarty P. A systematic review and meta-analysis of DNA methylation levels and imprinting disorders in children conceived by IVF/ICSI compared with children conceived spontaneously. *Hum Reprod Update* 2014;(20):840-52.
4. Pinborg A, Wennerholm UB, Romundstad LB, Loft A, Aittomaki K, Soderstrom-Anttila V, et al. Why do singletons conceived after assisted reproduction technology have adverse perinatal outcome? Systematic review and meta-analysis. *Hum Reprod Update* 2013;(19):87-104.
5. Qin J, Liu X, Sheng X, Wang H, and Gao S. Assisted reproductive technology and the risk of pregnancy-related complications and adverse pregnancy outcomes in singleton pregnancies: a meta-analysis of cohort studies. *Fertil Steril* 2016;(105):73-85 e1-6.
6. Zhu L, Zhang Y, Liu Y, Zhang R, Wu Y, Huang Y, et al. Maternal and Live-birth Outcomes of Pregnancies following Assisted Reproductive Technology: A Retrospective Cohort Study. *Sci Rep* 2016;(6):35141.
7. Choux C, Carmignac V, Bruno C, Sagot P, Vaiman D, and Fauque P. The placenta: phenotypic and epigenetic modifications induced by Assisted Reproductive Technologies throughout pregnancy. *Clin Epigenetics* 2015;(7):87.
8. Angiolini E, Fowden A, Coan P, Sandovici I, Smith P, Dean W, et al. Regulation of placental efficiency for nutrient transport by imprinted genes. *Placenta* 2006;(27 Suppl A):S98-102.
9. Ferguson-Smith AC, Moore T, Detmar J, Lewis A, Hemberger M, Jammes H, et al. Epigenetics and imprinting of the trophoblast -- a workshop report. *Placenta* 2006;(27 Suppl A):S122-6.
10. Monk D. Genomic imprinting in the human placenta. *Am J Obstet Gynecol* 2015;(213):S152-62.
11. Bannister AJ and Kouzarides T. Regulation of chromatin by histone modifications. *Cell Res* 2011;(21):381-95.
12. Portha B, Fournier A, Kioon MD, Mezger V, and Movassat J. Early environmental factors, alteration of epigenetic marks and metabolic disease susceptibility. *Biochimie* 2014;(97):1-15.
13. Rugg-Gunn PJ. Epigenetic features of the mouse trophoblast. *Reprod Biomed Online* 2012;(25):21-30.
14. Kohan-Ghadr HR, Kadam L, Jain C, Armant DR, and Drewlo S. Potential role of epigenetic mechanisms in regulation of trophoblast differentiation, migration, and invasion in the human placenta. *Cell Adh Migr* 2016;(10):126-35.
15. Eddy AC, Chapman H, and George EM. Acute Hypoxia and Chronic Ischemia Induce Differential Total Changes in Placental Epigenetic Modifications. *Reprod Sci* 2018:1933719118799193.
16. Rahat B, Mahajan A, Bagga R, Hamid A, and Kaur J. Epigenetic modifications at DMRs of placental genes are subjected to variations in normal gestation, pathological conditions and folate supplementation. *Sci Rep* 2017;(7):40774.
17. Barouki R, Melen E, Herceg Z, Beckers J, Chen J, Karagas M, et al. Epigenetics as a mechanism linking developmental exposures to long-term toxicity. *Environ Int* 2018;(114):77-86.
18. Choux C, Binqet C, Carmignac V, Bruno C, Chapusot C, Barberet J, et al. The epigenetic control of transposable elements and imprinted genes in newborns is affected by the mode of conception: ART versus spontaneous conception without underlying infertility. *Hum Reprod* 2018;(33):331-340.

19. Monk D, Morales J, den Dunnen JT, Russo S, Court F, Prawitt D, et al. Recommendations for a nomenclature system for reporting methylation aberrations in imprinted domains. *Epigenetics* 2018;(13):117-121.
20. Umlauf D, Goto Y, Cao R, Cerqueira F, Wagschal A, Zhang Y, et al. Imprinting along the Kcnq1 domain on mouse chromosome 7 involves repressive histone methylation and recruitment of Polycomb group complexes. *Nat Genet* 2004;(36):1296-300.
21. Jahangiri M, Shahhoseini M, and Movaghar B. H19 and MEST gene expression and histone modification in blastocysts cultured from vitrified and fresh two-cell mouse embryos. *Reprod Biomed Online* 2014;(29):559-66.
22. Monk D, Arnaud P, Apostolidou S, Hills FA, Kelsey G, Stanier P, et al. Limited evolutionary conservation of imprinting in the human placenta. *Proc Natl Acad Sci U S A* 2006;(103):6623-8.
23. Rousseau T, Ferdynus C, Quantin C, Gouyon JB, and Sagot P. [Liveborn birth-weight of single and uncomplicated pregnancies between 28 and 42 weeks of gestation from Burgundy perinatal network]. *J Gynecol Obstet Biol Reprod (Paris)* 2008;(37):589-96.
24. Thompson JM, Irgens LM, Skjaerven R, and Rasmussen S. Placenta weight percentile curves for singleton deliveries. *BJOG* 2007;(114):715-20.
25. Katari S, Turan N, Bibikova M, Erinle O, Chalian R, Foster M, et al. DNA methylation and gene expression differences in children conceived in vitro or in vivo. *Hum Mol Genet* 2009;(18):3769-78.
26. Nelissen EC, Dumoulin JC, Daunay A, Evers JL, Tost J, and van Montfoort AP. Placentas from pregnancies conceived by IVF/ICSI have a reduced DNA methylation level at the H19 and MEST differentially methylated regions. *Hum Reprod* 2013;(28):1117-26.
27. Rancourt RC, Harris HR, and Michels KB. Methylation levels at imprinting control regions are not altered with ovulation induction or in vitro fertilization in a birth cohort. *Hum Reprod* 2012;(27):2208-16.
28. Camprubi C, Iglesias-Platas I, Martin-Trujillo A, Salvador-Alarcon C, Rodriguez MA, Barredo DR, et al. Stability of genomic imprinting and gestational-age dynamic methylation in complicated pregnancies conceived following assisted reproductive technologies. *Biol Reprod* 2013;(89):50.
29. Turan N, Katari S, Gerson LF, Chalian R, Foster MW, Gaughan JP, et al. Inter- and intra-individual variation in allele-specific DNA methylation and gene expression in children conceived using assisted reproductive technology. *PLoS Genet* 2010;(6):e1001033.
30. Jahangiri M, Shahhoseini M, and Movaghar B. The Effect of Vitrification on Expression and Histone Marks of Igf2 and Oct4 in Blastocysts Cultured from Two-Cell Mouse Embryos. *Cell J* 2018;(19):607-613.
31. Li T, Vu TH, Ulaner GA, Littman E, Ling JQ, Chen HL, et al. IVF results in de novo DNA methylation and histone methylation at an Igf2-H19 imprinting epigenetic switch. *Mol Hum Reprod* 2005;(11):631-40.
32. Arnold DR, Gaspar RC, da Rocha CV, Sangalli JR, de Bem THC, Correa CAP, et al. Nuclear transfer alters placental gene expression and associated histone modifications of the placental-specific imprinted gene pleckstrin homology-like domain, family A, member 2 (PHLDA2) in cattle. *Reprod Fertil Dev* 2017;(29):458-467.
33. Fortier AL, Lopes FL, Darricarrere N, Martel J, and Trasler JM. Superovulation alters the expression of imprinted genes in the midgestation mouse placenta. *Hum Mol Genet* 2008;(17):1653-65.
34. Fortier AL, McGraw S, Lopes FL, Niles KM, Landry M, and Trasler JM. Modulation of imprinted gene expression following superovulation. *Mol Cell Endocrinol* 2014;(388):51-7.
35. Moore GE, Ishida M, Demetriou C, Al-Olabi L, Leon LJ, Thomas AC, et al. The role and interaction of imprinted genes in human fetal growth. *Philos Trans R Soc Lond B Biol Sci* 2015;(370):20140074.

36. Hamad MF. Quantification of histones and protamines mRNA transcripts in sperms of infertile couples and their impact on sperm's quality and chromatin integrity. *Reprod Biol* 2019;(19):6-13.
37. Stivnicka M, Garcia-Alvarez O, Ulcova-Galova Z, Sutovsky P, Abril-Parreno L, Dolejsova M, et al. H3K4me2 accompanies chromatin immaturity in human spermatozoa: an epigenetic marker for sperm quality assessment. *Syst Biol Reprod Med* 2019:1-9.

Figures legends

Figure 1: Flowchart.

From our precedent study [18], we selected the patients from IVF/ICSI group who presented with below the 5th percentile of percentage methylation for at least one of the studied DMRs (*H19* DMR, *KCNQ1OT1* DMR and *SNURF*). The 16 selected patients were then matched for 16 controls from the natural conception group for parity, new-born's sex, and gestational age at delivery.

Figure 2: Mapping of histone marks in placenta for each region of interest

For each region of interest (*H19* DMR (A), *KCNQ1OT1* DMR (B) and *SNURF* DMR (C)), we marked in green the sequence amplified by the qRT-PCR ChIP primers. To ensure the PCR amplified intervals mapping to the imprinted DMRs were enriched for the histone modification of interest, we performed an *in-silico* analysis to ensure primer design coincided with the largest peaks in placenta-derived ChIP-seq datasets. We used the Gene Expression Omnibus (GEO) application, available at <https://www.ncbi.nlm.nih.gov/geo/>. The GEO accession numbers for H3K4me3, H3K4me2, H3K9ac, and H3K9me3 were GSM1160199 (Histone H3K4me3 ChIP-Seq of Fetal Placenta), GSM753439 (ChIP-Seq Analysis of H3K4me2 in BMP4 Trophoblast Cells), GSM818049 (ChIP-Seq Analysis of H3K9ac in BMP4 Trophoblast Cells) and GSM1160204 (Histone H3K9me3 ChIP-Seq of Fetal Placenta), respectively. In parallel, normalized precipitation levels obtained in the 16 control samples of our cohort are displayed for each studied region. Precipitation levels of permissive marks H3K4me3, H3K4me2 and H3K9ac were normalized on precipitation levels of the *KLF10* gene whereas repressive marks H3K9me3 and H3K9me2 were normalized on the satellite region *SAT4*.

Figure 3: Histone post-translational modifications are imprinted in the placenta

For each region of interest, an informative SNP was selected, the control DNA was genotyped, and heterozygous samples were studied. DNA was digested by HpaII and BstUI before sequencing to evidence the methylated allele. Then the ChIP products were also sequenced to assess which allele was the most represented in either permissive or repressive marks. It appears that the unmethylated allele is mostly represented in the permissive marks H3K4me3, H3K4me2 and H3K9ac. On the contrary, the methylated allele is mostly represented in the repressive marks H3K9me3 and H3K9me2. Thus methylated regions are associated with repressive histone marks whereas unmethylated regions are associated with permissive histone marks.

Figure 4: Comparisons between IVF/ICSI group and controls.

DNA methylation levels were lower in the IVF/ICSI group than in the natural conception group (A), some repressive and permissive marks normalized precipitation levels were lower and higher, respectively, in the IVF/ICSI group compared to the natural conception group (B and C, respectively).

Each box represents the interquartile range (IQR). Lines inside the boxes are the median. Whiskers represent the 10th and 90th percentiles. Crosses represent the mean. For the histone marks profiling, the figures present the ratio between the % of input obtained at the region of interest and the % of input obtained at the control region. IVF: *In Vitro* Fertilization, ICSI: IVF with Intra Cytoplasmic Sperm Injection, ns: non-significant. Nat.: natural conception group.

Tables

Table 1. Population characteristics

	Natural Conception (n = 16)	IVF/ICSI (n = 16)	P
Maternal characteristics			
Age (years)	28.5 +/- 4.2	31.3 +/- 6.3	0.137
Pre-pregnancy parity	0 [0 - 0.5]	0 [0 - 0.5]	0.980
Tobacco Smoking	2 (1.3%)	1 (6.3%)	1
Pre-pregnancy BMI (kg/m ²)	21.7 +/- 2.8	24.6 +/- 4.8	0.050
Paternal characteristics			
Age (years)	30.7 +/- 5.8	32.8 +/- 5.5	0.306
Tobacco smoking	3 (1.9%)	5 (3.1%)	0.685
New-born characteristics			
Term (weeks of gestation)	39.7 +/- 1.1	38.9 +/- 2.1	0.194
Birth weight (grams)	3310.9 +/- 461.6	3184.1 +/- 593.7	0.505
z-score of birth weight	0.06 +/- 1.13	0.10 +/- 1.23	0.930
Placenta weight (grams)	483.4 +/- 109.1	517.8 +/- 135.1	0.435
z-score of placenta weight	-1.39 +/- 0.82	-1.02 +/- 0.93	0.235
Sex ratio M/F [95 % CI]	0.60 [0.43 - 0.77]	0.60 [0.43 - 0.77]	1

Results are displayed as: n (%), mean ± standard deviation, or median [interquartile range] and compared with Student's test or Mann-Whitney according to the distribution, significant results in bold, BMI: body mass index

Table 2. DNA methylation and expression according to the mode of conception

Methylation	Expression
-------------	------------

	Natural conception	IVF/ICSI	P	Natural conception	IVF/ICSI	P
Imprinted genes						
<i>H19/IGF2</i>	53.54 [49.59-59.29]	45.09 [43.16-48.94]	0.004	228.34 [186.14-350.50]	301.83 [173.01-506.40]	0.395
<i>KCNQ1OT1</i>	39.38 [34.76-41.94]	32.79 [31.70-35.73]	0.001	0.06 [0.05-0.11]	0.06 [0.04-0.23]	0.594
<i>SNURF</i>	41.20 [38.41-42.09]	38.30 [35.54-40.47]	0.036	0.23 [0.09-0.31]	0.29 [0.11-0.54]	0.244

Results are displayed as median [interquartile range]. P-values are the result of Student or Mann-Whitney test, as recommended according to the distribution

Figure 1

Figure 2

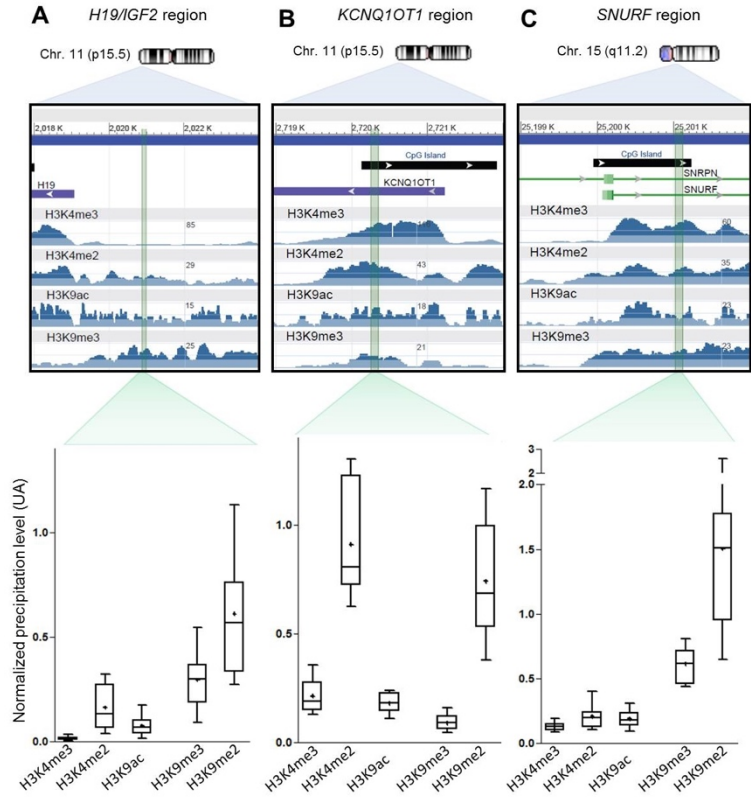


Figure 3

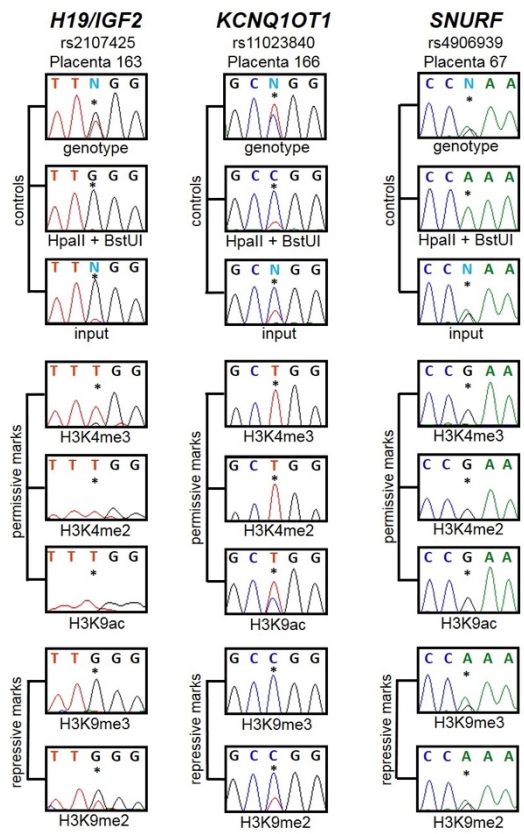
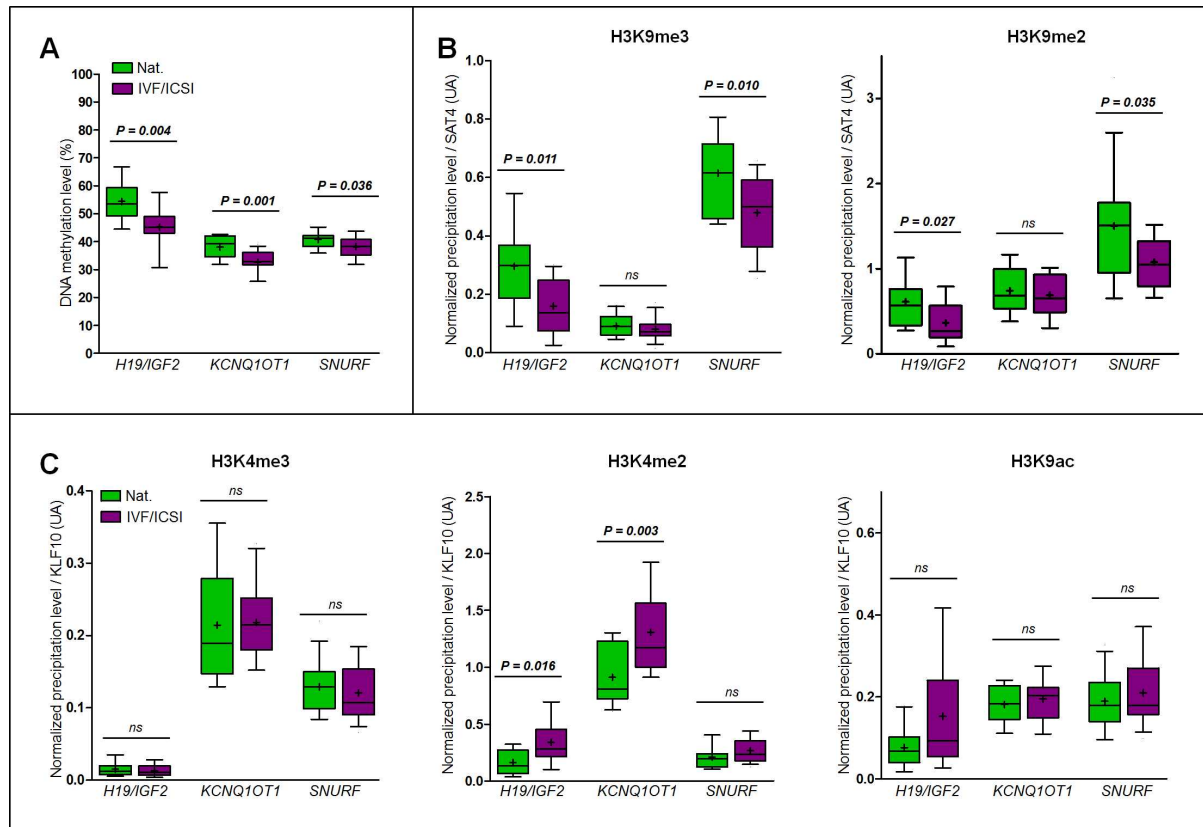


Figure 4



Supplementary material

Table S1: Primers for sequencing

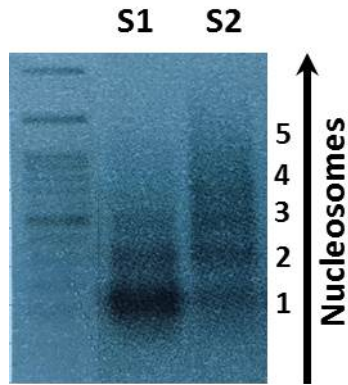
Region	Data base Reference	Sequence Number Nucleotide position	Primers (sequencing primer in bold)	Product Reaction temperature
Imprinted genes				
<i>H19/IGF2: IG-DMR</i>	UCSC	hg38: chr11:1,997,582-2,003,510	F: GGGCTGTCCTTAGACGGAGTC R: GTATTTCTGGAGGCTTCTCC	409 pb 56°C
<i>KCNQ1OT1: TSS-DMR</i>	UCSC	hg38 : chr11:2,698,718-2,701,029	F: GATGCCACCCGGGCTCAGATTGG R: ACCCCGGGGTGGTGAACACATCA	216 pb 56°C
<i>SNURF: TSS-DMR</i>	UCSC	hg38 : chr15:24,954,857-24,956,829	F: ACTGCGCCACAACCGGAAAGGAA R: GTAGAGCCGCCAGTGGGAGGG	320 pb 56°C

Bioline products were used for the PCR mix as follows: water 11.55 µL, 5M betaine 7.5 µL, 10xNH4 Reaction Buffer 2.5 µL, 50 mM MgCl₂ 0.75 µL, 2 mM dNTP 0.5 µL, BIOTAQ DNA polymerase 5U/µL 0.2 µL, with 1 µL DNA and 2 ng/µL of each primer, for a final volume of 25 µL. Amplification was performed with the following conditions: 5 min denaturation phase at 96°C, followed by 40 cycles of three steps: 30 s denaturation at 96°C, 30 s annealing at 56°C and 30 s extension at 72°C with final extension 7 min at 72°C.

Table S2: Primers for qRT-PCR CHIP

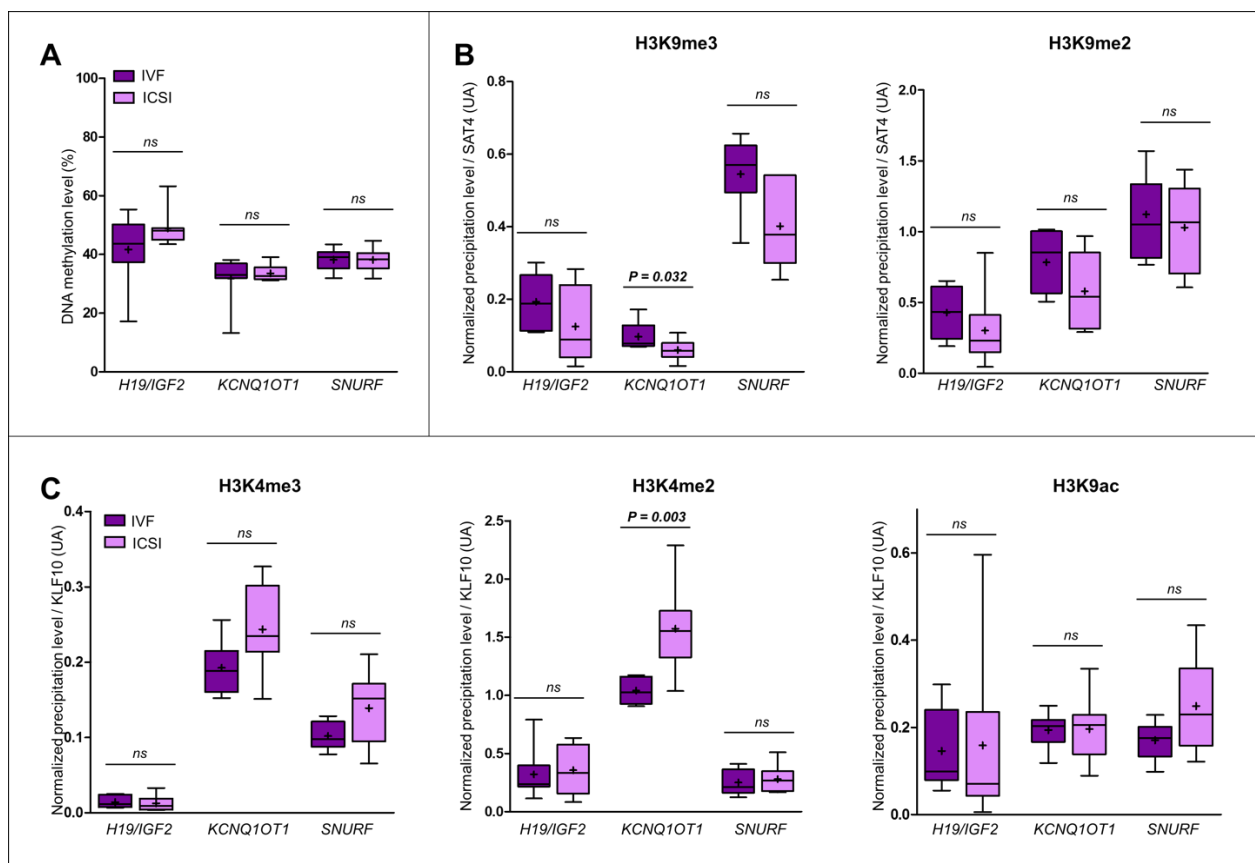
Region	Data base Reference	Sequence Number Nucleotide position	Primers	Product Reaction temperature
Housekeeping genes				
<i>KLF10</i>	Ensembl	Ensembl ENSG00000155090 hg 38: chr 8:102,648,779-102,655,902 reverse strand	F: GACAAGACCAGGCGAGGAAG R: GCCAACCATGCTCAACTTCG	89 pb 60°C
<i>SATα chr4</i>	NCBI Alexiadis <i>et al.</i> , 2017	M38467	F: CTGCACTACCTGAAGAGGAC R: GATGGTTCAACTCTTACA	139 pb 60°C
Imprinted genes				
<i>H19/IGF2: IG-DMR</i>	UCSC	hg38: chr11:1,997,582-2,003,510	F: AGCTGTGCTCTGGATAGATG R: ATGATCACAGTGTGTTCCACC	60 pb 60°C
<i>KCNQ1OT1: TSS-DMR</i>	UCSC	hg38 : chr11:2,698,718-2,701,029	F: ATTTCCGACTCCGGTCCCAA R: CATCGTGGTTCTGAGTCCGC	94 pb 60°C
<i>SNURF: TSS-DMR</i>	UCSC	hg38 : chr15:24,954,857-24,956,829	F: CTGTGCTACTGCCCTTCTG R: GGAGTGACTAAGGGACGCTGAATG	68 pb 60°C

4.5 µL 2X SYBR™ Green PCR Master Mix (Applied) was used with 0.1 µL primers (0.1 µg/µL), 0.4 µL water and 5 µL DNA (diluted 1/40), for a final volume of 10 µL. Amplification was performed in triplicate using QuantStudio™ 5 Real-Time PCR system (Applied Biosystems™) with the following conditions: 10 min denaturation phase at 95°C, followed by 40 cycles of two steps: 15 s denaturation at 95°C and 1 min annealing/extension at 60°C.



Supplemental Figure 1: Nucleosome ladder

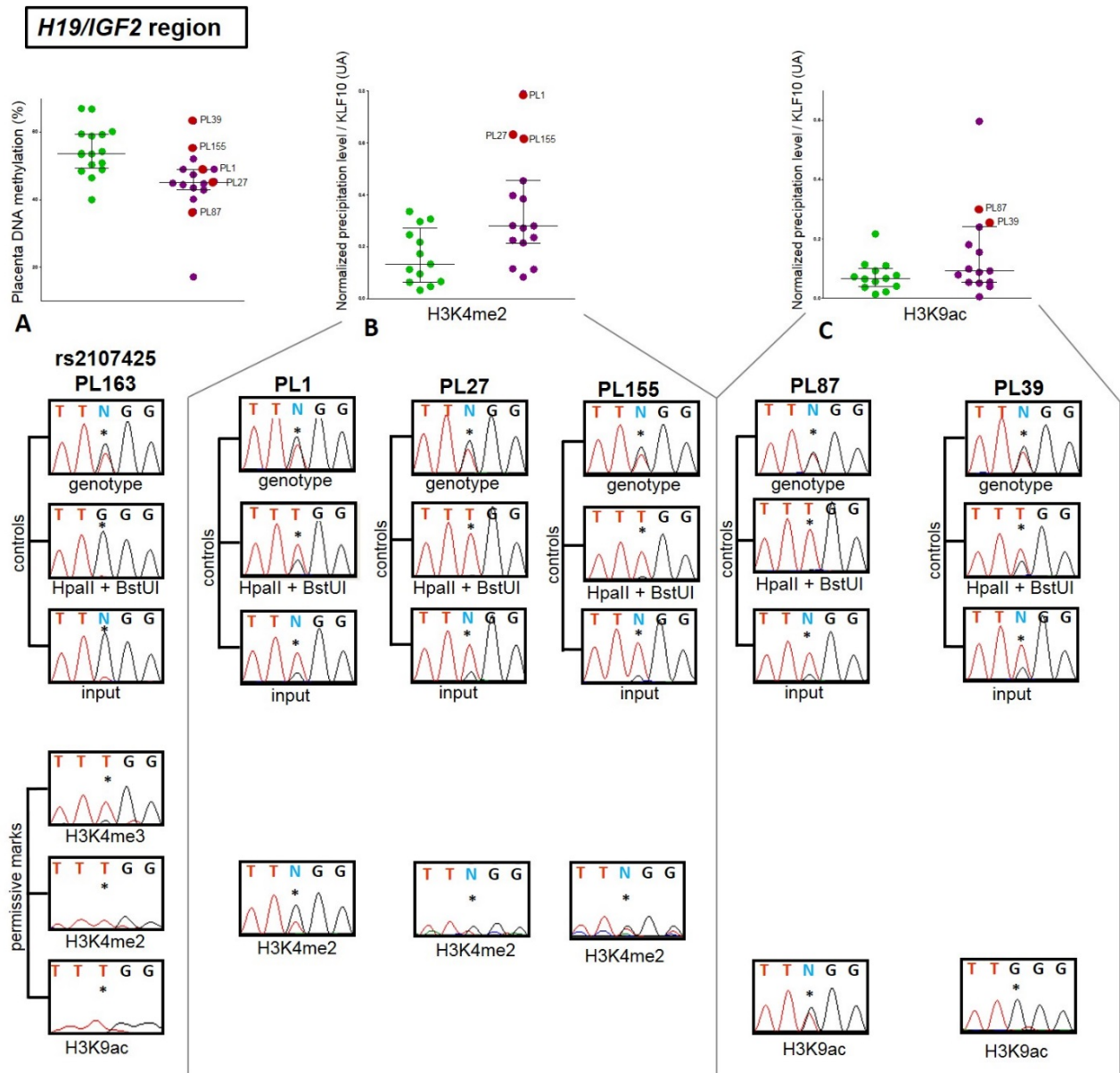
100 μ L of each fraction of chromatin S1 and S2 were cleaned and migrated on an agarose gel. Then the gel was immersed in a midori green bath during 2 hours. S1 chromatin fraction was mostly composed of mono and di nucleosomes whereas S2 fraction contained mostly fragments of 2 to 5 nucleosomes.



Supplemental Figure 2: Comparisons between conventional IVF and ICSI.

DNA methylation levels were not significantly different between both groups (A), some repressive and permissive marks normalized precipitation levels were lower and higher, respectively, in the ICSI group compared to IVF group (B and C, respectively).

Each box represents the interquartile range (IQR). Lines inside the boxes are the median. Whiskers represent the 10th and 90th percentiles. Crosses represent the mean. For the histone marks profiling, the figures present the ratio between the % of input obtained at the region of interest and the % of input obtained at the control region. IVF: *In Vitro* Fertilization, ICSI: IVF with Intra Cytoplasmic Sperm Injection, ns: non-significant.

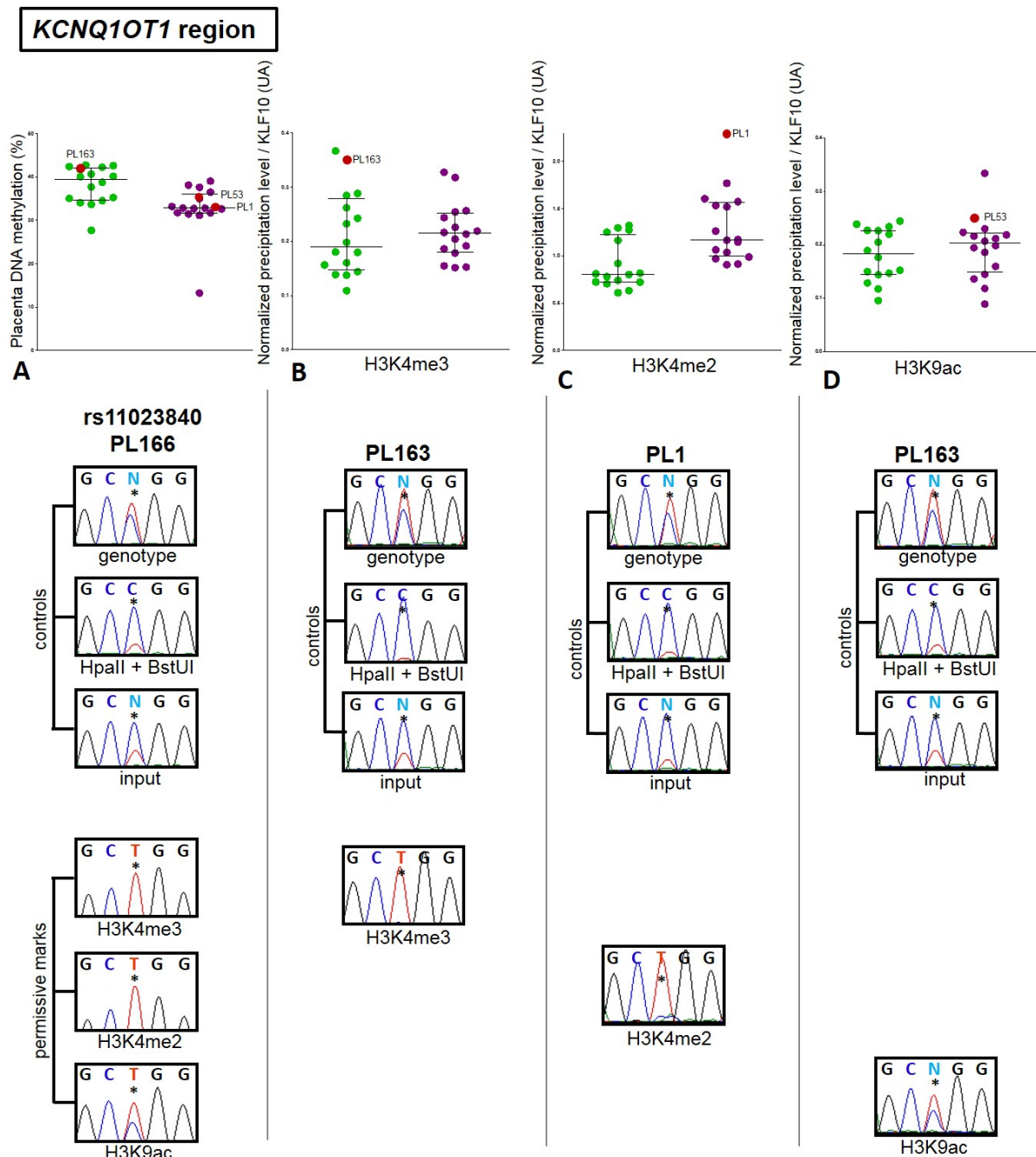


Supplemental Figure 3: Analysis of the outliers in the *H19/IGF2* region

A: Placental DNA methylation of IVF/ICSI group (in purple) vs. natural conception group (in green). Bars represent the median with the interquartile range. The outliers studied are marked with red dots. PL163 represents the control placenta at the SNP rs2107425 of this region. Sequencing of cDNA (genotyping), DNA digested with HpaII and input chromatin for ChIP and chromatin precipitated with permissive histone marks H3K4me3, H3K4me2 and H3K9ac are displayed.

B: Precipitation levels of H3K4me2 normalized on KLF10, with the 3 outliers studied marked with red dots (PL1, 27 and 155). Sequencing of the 3 outliers for controls (genotype, HpaII and input) and for H3K4me2

C: Precipitation levels of H3K9ac normalized on KLF10, with the 2 outliers studied marked with red dots (PL87 and 39). Sequencing of the 2 outliers for controls (genotype, HpaII and input) and for H3K9ac



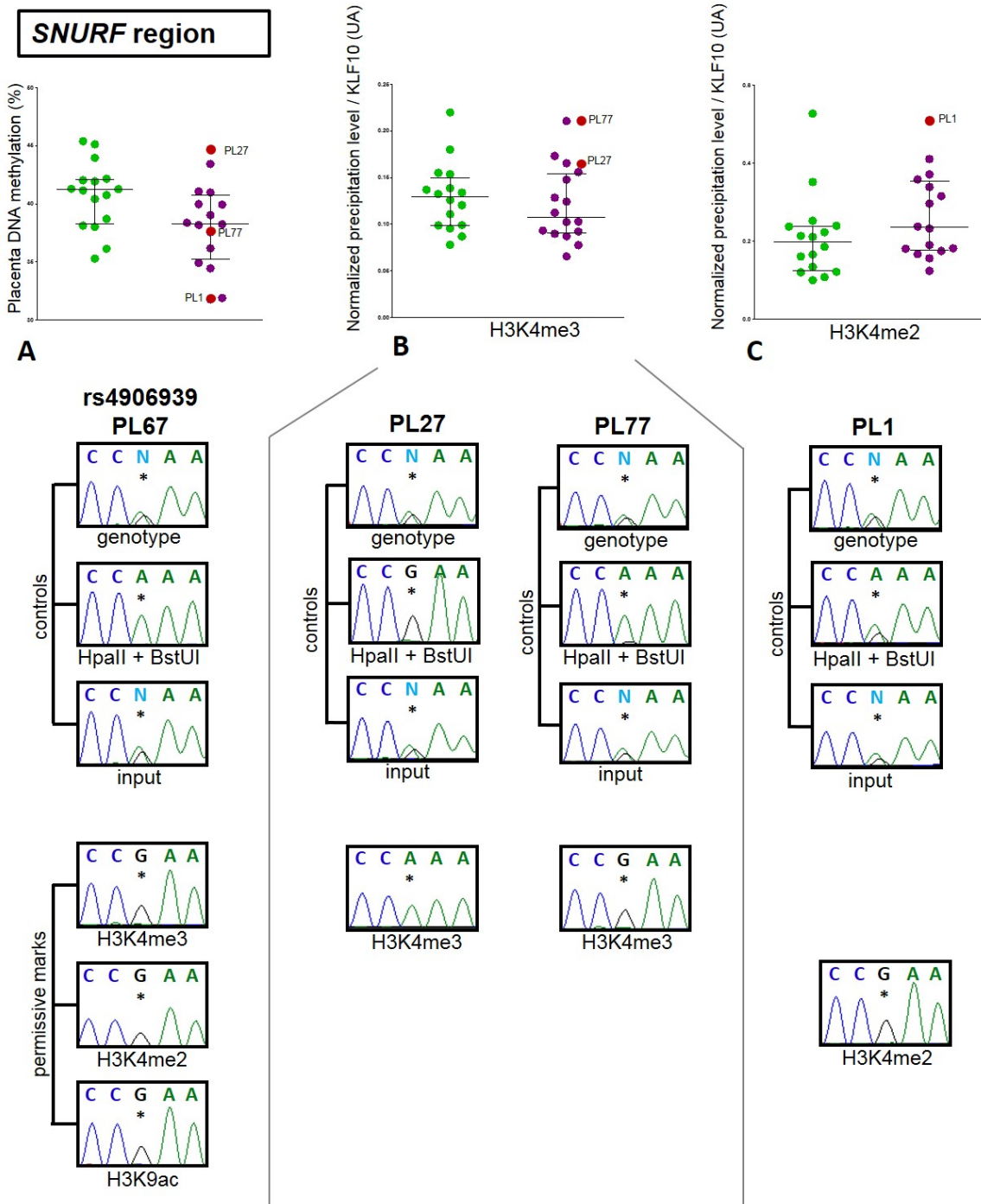
Supplemental Figure 4: Analysis of the outliers in the *KCNQ1OT1* region

A: Placental DNA methylation of IVF/ICSI group (in purple) vs. natural conception group (in green). Bars represent the median with the interquartile range. The outliers studied are marked with red dots. PL166 represents the control placenta at the SNP rs11023840 of this region. Sequencing of cDNA (genotyping), DNA digested with HpaI and BstUI and input chromatin for ChIP and chromatin precipitated with permissive histone marks H3K4me3, H3K4me2 and H3K9ac are displayed.

B: Precipitation levels of H3K4me3 normalized on KLF10, with the outlier studied marked with red dot (PL163). Sequencing of the outlier for controls (genotype, HpaI + BstUI and input) and for H3K4me3

C: Precipitation levels of H3K4me2 normalized on KLF10, with the outlier studied marked with red dot (PL1). Sequencing of the outlier for controls (genotype, HpaI + BstUI and input) and for H3K4me2

D: Precipitation levels of H3K9ac normalized on KLF10, with the outlier studied marked with red dot (PL163). Sequencing of the outlier for controls (genotype, HpaI and input) and for H3K9ac



Supplemental Figure 5: Analysis of the outliers in the *SNURF* region

A: Placental DNA methylation of IVF/ICSI group (in purple) vs. natural conception group (in green). Bars represent the median with the interquartile range. The outliers studied are marked with red dots. PL67 represents the control placenta at the SNP rs4906939 of this region. Sequencing of cDNA (genotyping), DNA digested with HpaII and BstUI and input chromatin for ChIP and chromatin precipitated with permissive histone marks H3K4me3, H3K4me2 and H3K9ac are displayed.

B: Precipitation levels of H3K4me3 normalized on KLF10, with the outliers studied marked with red dots (PL27 and 77). Sequencing of the outliers for controls (genotype, HpaII + BstUI and input) and for H3K4me3

C: Precipitation levels of H3K4me2 normalized on KLF10, with the outlier studied marked with red dot (PL1). Sequencing of the outlier for controls (genotype, HpaII + BstUI and input) and for H3K4me2